Bioleaching of chalcopyrite and bornite by moderately thermophilic bacteria: an emphasis on their interactions

Hong-bo Zhao[1,2], *Jun Wang*[1,2], *Xiao-wen Gan*[1,2], *Wen-qing Qin*[1,2], *Ming-hao Hu*[1,2], *and Guan-zhou Qiu*[1,2]

1) School of Minerals Processing & Bioengineering, Central South University, Changsha 410083, China
2) Key Lab of Bio-hydrometallurgy of the Ministry of Education, Changsha 410083, China

Abstract: Interactions between chalcopyrite and bornite during bioleaching by moderately thermophilic bacteria were investigated mainly by X-ray diffraction, scanning electron microscopy, and electrochemical measurements performed in conjunction with bioleaching experiments. The results showed that a synergistic effect existed between chalcopyrite and bornite during bioleaching by both *Acidithiobacillus caldus* and *Leptospirillum ferriphilum* and that extremely high copper extraction could be achieved when chalcopyrite and bornite coexisted in a bioleaching system. Bornite dissolved preferentially because of its lower corrosion potential, and its dissolution was accelerated by the galvanic current during the initial stage of bioleaching. The galvanic current and optimum redox potential of 390–480 mV vs. Ag/AgCl promoted the reduction of chalcopyrite to chalcocite (Cu_2S), thus accelerating its dissolution.

Keywords: chalcopyrite; bornite; bioleaching; interactions; redox potential

1. Introduction

Chalcopyrite ($CuFeS_2$) and bornite (Cu_5FeS_4) are the most abundant copper-bearing minerals in the world [1–3]. Smelting is still the major process used to extract copper from these two primary copper sulfide minerals. The hydrometallurgical processes, especially the bio-hydrometallurgical processes, have been successfully applied to the processing of secondary copper sulfide minerals, and hydrometallurgical technology is more promising than smelting because it is simpler, more efficient, and more eco-friendly. However, chalcopyrite and bornite are too refractory to be treated using bio-hydrometallurgical methods [4–5].

Chalcopyrite and bornite usually coexist in raw ores; thus, their interaction and relationship during dissolution processes are an important and valuable research topic. Some researchers [6–9] have reported that chalcopyrite is reduced to bornite during the initial stage of bioleaching and that this first step is also the rate-limiting step. Acres *et al.* [10] observed that bornite can decrease the oxidation rate of chal-

copyrite and can also slow its leaching rate in the presence of hydrochloric acid.

Different strains of microorganisms can result in different dissolution efficiencies and dissolution pathways in the bioleaching of sulfide minerals, and three main types of microorganisms can be classified according to their optimum growth temperature: mesophiles, moderately thermophilic bacteria, and extremely thermophilic bacteria. Extremely thermophilic bacteria are sensitive to high shear force at high pulp density because of the absence of a cell wall, which restricts their further industrial application [11–12]. Mesophiles can easily cause the passivation of chalcopyrite and result in low copper extraction. Moderately thermophilic bacteria, in contrast, have extensive application prospects because of their advantages in accelerating the dissolution of chalcopyrite and in inhibiting the formation of passivation layer [12–14].

Therefore, in the present work, the bioleaching of chalcopyrite and bornite in the presence of moderately thermophilic bacteria *Acidithiobacillus caldus* (*A. caldus*) and *Lep-*

Springer

tospirillum ferriphilum (*L. ferriphilum*) was conducted to investigate the interactions between chalcopyrite and bornite.

2. Experimental

2.1. Minerals and reagents

Chalcopyrite samples were obtained from the Geological Museum of Guangxi Province, China, and bornite samples were obtained from Meizhou, Guangdong Province, China. X-ray diffraction (XRD) analysis (Fig. 1) indicated that the samples were extremely pure. Chemical analysis showed that the chalcopyrite sample contained 34.46wt% Cu, 31.53wt% Fe, and 33.12wt% S and that the bornite sample contained 61.59wt% Cu, 10.04wt% Fe, and 27.10wt% S. Copper concentrates were obtained via the flotation process, and XRD analysis (Fig. 1) confirmed that the chalcopyrite and bornite were the main mineralogical compositions. Elemental analysis indicated that the copper concentrates mainly contained 40.23wt% Cu, 24.00wt% Fe, and 32.53wt% S. Ore samples were ground and sieved to less than 0.074 mm before being used for bioleaching experiments. High-purity chalcopyrite and bornite samples were cut into cylindrical electrodes with a diameter of approximately 1.5 cm, a thickness of approximately 5 mm, and an area of 1 cm^2. All of the chemicals used in this work were of analytical grade.
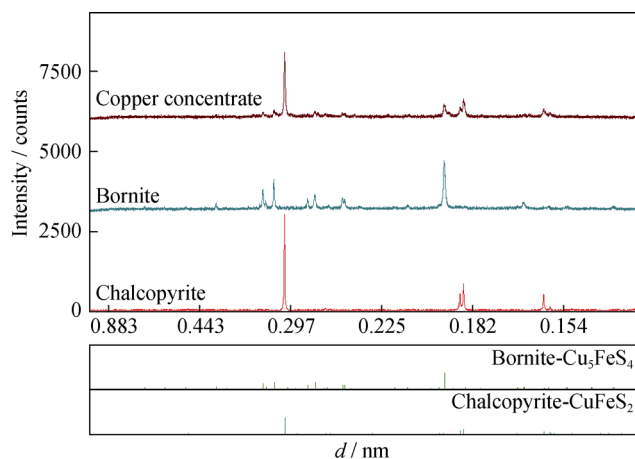

Fig. 1. Mineralogical composition analysis (XRD) results of untreated chalcopyrite, bornite, and copper concentrates.

2.2. Microorganisms and culture conditions

Moderately thermophilic bacteria, including *A. caldus* and *L. ferriphilum*, were obtained from the Key Lab of Biohydrometallurgy of the Ministry of Education, Central South University, Changsha, China. The bacteria were cultured in a bacteria culture medium consisting of $(NH_4)_2SO_4$

(3.0 g/L), $MgSO_4·7H_2O$ (0.5 g/L), K_2HPO_4 (0.5 g/L), KCl (0.1 g/L), and $Ca(NO_3)_2$ (0.01 g/L). The temperature and pH value were maintained at 45°C and 1.70, respectively. *A. caldus* and *L. ferriphilum* were sub-cultured into a basal salts medium supplemented with 10 g/L sulfur and 44.7 g/L ferrous sulfate $(FeSO_4·7H_2O)$ as the energy sources, respectively. The resulting culture was used as inocula for the bioleaching experiments.

2.3. Bioleaching experiments

For bioleaching of chalcopyrite and bornite, a 250-mL shake flask containing 90 mL of bacteria culture medium, 3 g of minerals with different mass ratios of chalcopyrite and bornite, and 10 mL of bacterial cultures was placed into an orbital shaker at 170 r/min and at 45°C; the pH value of the resulting mixture was regularly adjusted to 1.70 with sulfuric acid, and water lost by evaporation was supplemented periodically by adding deionized water. Bioleaching of copper concentrates was conducted in a 5-L stirred reactor containing 300 mL of bacterial cultures, 2700 mL of bacteria culture medium, and 90 g of copper concentrates. The culture medium was previously sterilized in an autoclave under a pressure of 0.1 MPa and a temperature of 121°C for 30 min. Mineral samples were sterilized by ultraviolet light. During all of the leaching processes, the pH meter and potentiometer were sterilized with ethyl alcohol. Cupric concentrations were monitored by inductively coupled plasma atomic emission spectrometry (ICP−AES) (America Baird Co. PS−6). The pH values were measured with a pH meter (PHSJ−4A), and the redox potentials of the leaching solution were measured using a Pt electrode with reference to an Ag/AgCl electrode (3.0 mol/L KCl) (BPP−922).

2.4. Electrochemical measurements

A conventional three-electrode system consisting of a working electrode, a graphite rod as the counter electrode, and an Ag/AgCl (3.0 mol/L KCl) electrode as the reference electrode was used in the electrochemical measurements. The working electrodes were polished with #3000 silicon carbide paper before each electrochemical measurement. The basic electrolyte was sterile bacteria culture medium; the pH value of the electrolyte was adjusted to 1.70 by adding sulfuric acid, and its temperature was maintained at 45°C. The electrochemical measurements were performed on a Princeton model 283 potentiostat (EG&G of Princeton Applied Research) coupled to a personal computer. Cyclic voltammetry (CV) tests were all conducted at a sweep rate of 20 mV/s, Tafel tests were performed at a sweep rate of 0.5 mV/s, and all of the potentiostatic tests were performed

for 240 s. All potential values in the present work are stated with reference to an Ag/AgCl electrode vs. Ag/AgCl.

2.5. XRD and SEM/EDS analysis

The mineralogical compositions of solid samples were examined by XRD (DX−2700). A scanning electron microscope (JSM−6360 LV) equipped with an energy-dispersive X-ray spectrometer was used to analyze the surface of solid samples. The leaching samples were filtered and rinsed with deionized water three times and were then dried in a vacuum drying oven (DZF−6050) before XRD and SEM/EDS analyses.

3. Results and discussion

3.1. Bioleaching experiments

Fig. 2 shows the bioleaching results for mixtures with different mass fractions of chalcopyrite and bornite. After 30 d of bioleaching with *A. caldus*, the copper extractions of individual chalcopyrite and individual bornite were 23% and 41%, respectively. However, the total copper extractions were 88%, 85%, and 70% for the mixtures with chalcopyrite-to-bornite mass ratios of 2.5:0.5, 1.5:1.5, and 0.5:2.5,

respectively. If bornite is assumed to be totally extracted from the aforementioned mixtures, the corresponding copper extractions of chalcopyrite are 83% and 58%, respectively. Similarly, if chalcopyrite is assumed to be totally extracted from the aforementioned mixtures, the corresponding copper extractions of bornite are calculated as 54%, 76%, and 66%, respectively. Thus, copper extractions of chalcopyrite and bornite both increased significantly when they were both present during bioleaching. Therefore, a synergistic effect existed between chalcopyrite and bornite during bioleaching in the presence of *A. caldus*. A more obvious synergistic effect was observed in bioleaching by *L. ferriphilum*, as shown in Fig. 2(b). The total copper extractions of all the mixtures containing chalcopyrite and bornite were greater than 90% after 30 d of bioleaching, compared to just 35% of individual chalcopyrite and 48% of individual bornite. If bornite is assumed to be totally extracted from the mixtures, the copper extractions of chalcopyrite are 93% and 72% for the 2.5:0.5 and 1.5:1.5 chalcopyrite-to-bornite mixtures, respectively. If chalcopyrite is assumed to be totally extracted from the mixtures, the copper extractions of bornite are 81%, 84%, and 88% for the 2.5:0.5, 1.5:1.5, and 0.5:2.5 chalcopyrite-to-bornite mixtures, respectively.
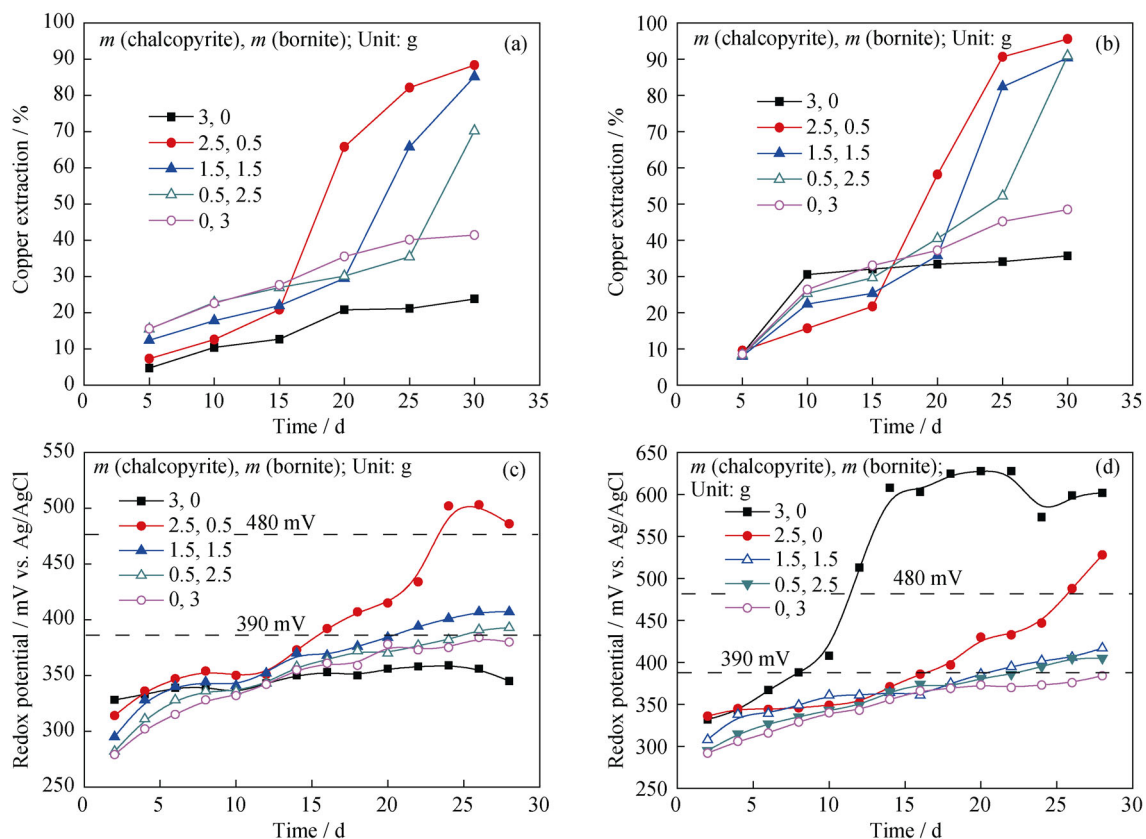

Fig. 2.   Bioleaching of chalcopyrite and bornite in shake flasks: (a) copper extraction (*A. caldus*); (b) copper extraction (*L. ferriphilum*); (c) redox potential (*A. caldus*); (d) redox potential (*L. ferriphilum*).

Therefore, chalcopyrite and bornite were promoted mutually during bioleaching, and a synergistic effect existed between chalcopyrite and bornite during bioleaching by *A. caldus* and by *L. ferriphilum*.

Figs. 2(c) and 2(d) present the changes of redox potential during bioleaching by *A. caldus* and by *L. ferriphilum*, respectively. The copper extractions of bioleaching of mixtures increased slowly when the redox potentials were less than 390 mV and started to increase sharply when the redox potentials reached approximately 390 mV. For bioleaching by *L. ferriphilum*, the copper extractions increased sharply when the redox potentials were greater than 390 mV, and the dissolution almost stagnated when the redox potentials exceeded 480 mV. The redox potential can be maintained within a certain range for a long period of time during bioleaching because of the blend of chalcopyrite and bornite.

An extremely high copper extraction greater than 90% was obtained from bioleaching of copper concentrates by *L. ferriphilum* (Fig. 3). Similarly, the copper extraction increased sharply when the redox potential exceeded 390 mV and stopped when the redox potential exceeded 480 mV.

The redox potential is considered an important factor, even a determining factor, in the leaching of chalcopyrite. Numerous researchers [7,15−18] have hypothesized that a relatively low redox potential facilitates the effective disso-

lution of chalcopyrite in the presence of bacteria or ferric sulfate and that extremely high redox potentials can easily cause passivation of chalcopyrite, thus inhibiting its further dissolution. Ahmadi *et al.* [19] used an electro-bioreactor to control the redox potential of a leaching solution during bioleaching of chalcopyrite flotation concentrates and observed that copper could be effectively extracted by controlling the redox potential between 400 and 425 mV vs. Ag/AgCl. Third *et al.* [16] controlled the redox potential of leaching solution by oxygen limitation during bioleaching of chalcopyrite and proposed that a constant redox potential (380 mV vs. Ag/AgCl) resulted in significantly greater copper extraction. Hiroyoshi *et al.* [20−21] proposed that chalcopyrite can be reduced to chalcocite (Cu_2S) in the presence of cupric ions and ferrous ions and that the formed chalcocite (Cu_2S) can be more amenable to oxidation than chalcopyrite. In the present work, the redox potentials during bioleaching of mixtures were maintained within the approximate range from 390 to 480 mV, which was considered an optimal range of redox potentials for the dissolution of chalcopyrite by numerous other researchers [15,17,19,22−26]. Therefore, the control of redox potential within a certain range of approximately 390 to 480 mV is likely one of the main causes of the synergistic bioleaching of chalcopyrite and bornite.
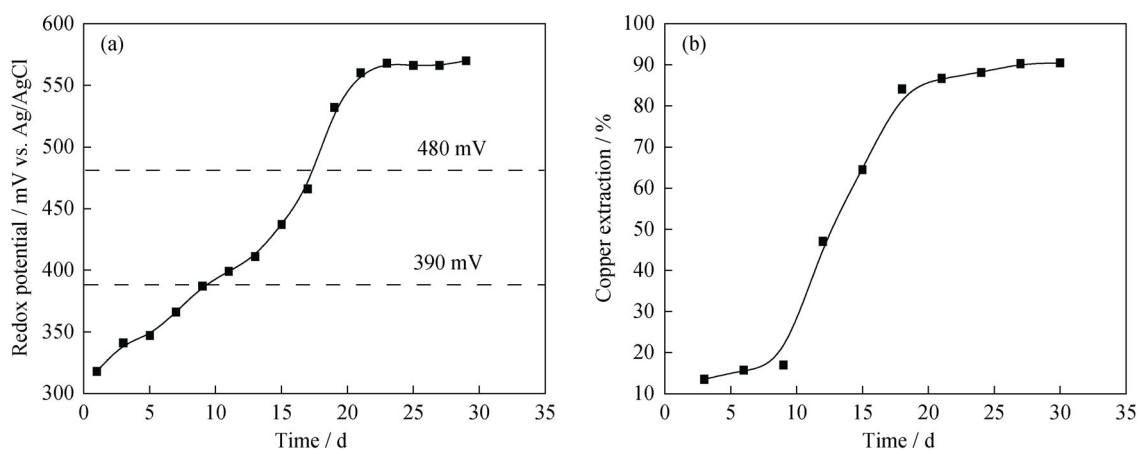

Fig. 3.   Bioleaching of copper concentrates containing chalcopyrite and bornite in a stirred reactor: (a) copper extraction; (b) redox potential vs. Ag/AgCl.

Fig. 4 presents the effects of cupric and ferrous ions on the redox potential of a leaching solution in the presence or absence of ferric ions. Fig. 4(a) indicates that a linear relationship exists between the redox potential and the logarithm of the concentration ratio of ferric ions to ferrous ions; the slope of the redox potential to the logarithm of the concentration ratio was approximately the same as the theoretical value calculated by the Nernst equation shown in Eq. (1),

thereby demonstrating that the redox potential was mainly determined by the concentration ratio of ferric ions to ferrous ions. Figs. 4(b), 4(c), and 4(d) show the effect of cupric ions on the potential of a solution in the absence of ferric ions. This figure reveals that the redox potential was determined primarily by the concentration of ferrous ions and that the influence of cupric ions on the redox potential can be ignored. Therefore, the redox potential during bioleach-

ing of a mixture containing chalcopyrite and bornite was controlled within an appropriate range mainly by controlling the concentrations of ferric ions and ferrous ions. The Nernst equation is as follows:

$$E = E^{\ominus} + \frac{RT}{F} \ln \frac{[\text{Fe}^{3+}]}{[\text{Fe}^{2+}]} \qquad (1)$$

where $E^{\ominus}$ is the standard potential, F is the Faraday constant, and R is the gas constant.
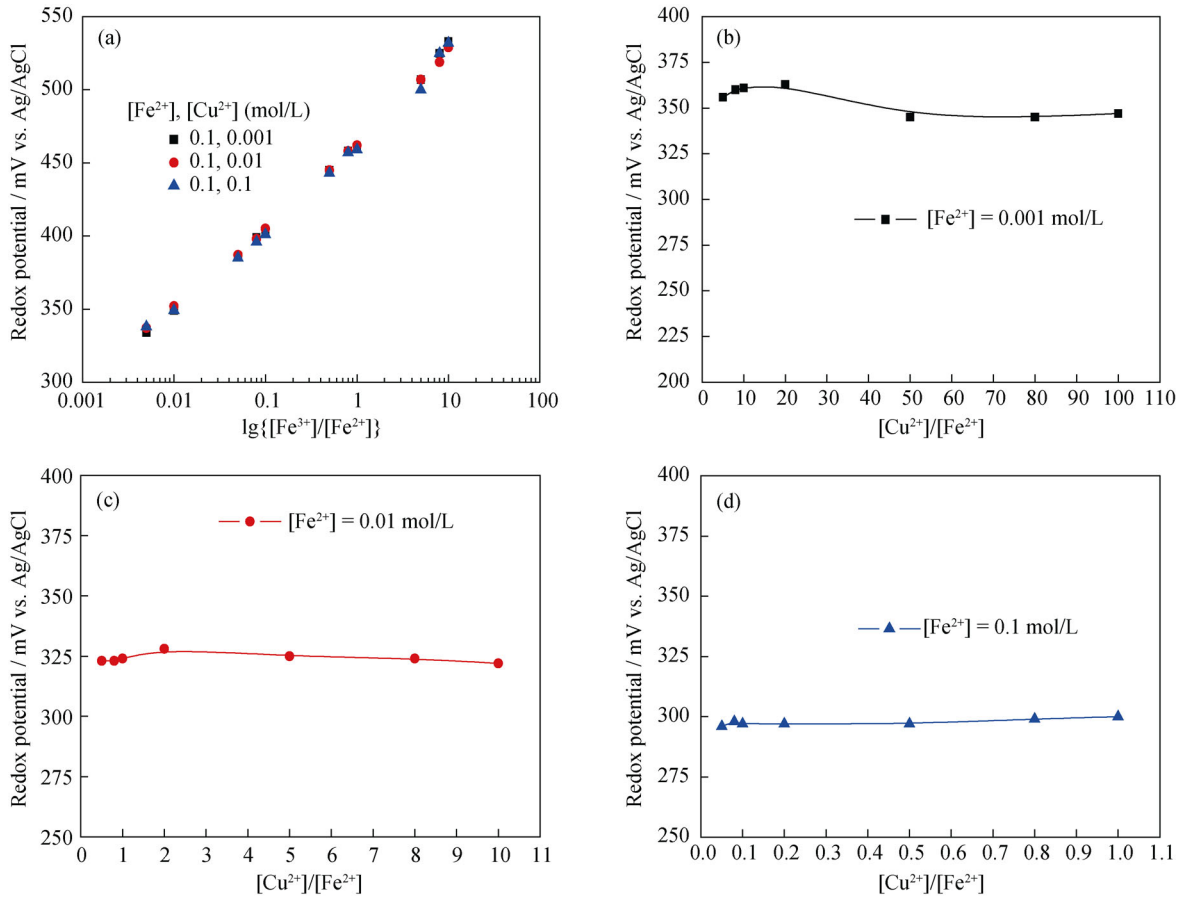

Fig. 4.   Effects of cupric ions on the redox potential of the leaching solution in the (a) presence or (b, c, d) absence of ferric ions.

To further investigate the intermediate species during bioleaching, XRD analysis was used to analyze the mineralogical phase transformation of a 1:1 chalcopyrite-to-bornite mixture after the mixture had been subjected to bioleaching for 5 or 20 d. Figs. 5(a) and 5(b) show the mineralogical compositions of the 1:1 mixture leached by *A. caldus* for 5 and 20 d, respectively. After just 5 d of bioleaching, bornite was totally extracted, whereas a large amount of chalcopyrite remained, indicating that bornite dissolved before chalcopyrite and that the dissolution of bornite was significantly accelerated by the addition of chalcopyrite. After 20 d of bioleaching, large amount of jarosite and elemental sulfur formed, but the copper extraction still increased sharply, indicating that jarosite and elemental sulfur did not significantly hinder the further dissolution of chalcopyrite. Similar results were obtained when the 1:1 mixture was bioleached by *L. ferriphilum* (Figs. 5(c) and 5(d)). Additionally, chal-

cocite (Cu_2S) was detected as the main intermediate species in the initial stage of bioleaching of the 1:1 mixture by both *A. caldus* and *L. ferriphilum*.

To further interpret the effect of jarosite and elemental sulfur on bioleaching of minerals, SEM analysis was utilized to analyze the surface of the 1:1 mixture leached for 20 d. Fig. 6(a) shows that numerous leaching products were adsorbed onto the mineral surfaces after 20 d of bioleaching by *A. caldus*; XRD analysis revealed that the adsorbed products consisted primarily of jarosite and elemental sulfur. However, the product film was loose and in the shape of floccules, which cannot effectively hinder the diffusion of reactants to the minerals' surface. Therefore, a significant amount of jarosite and elemental sulfur did not hinder the further dissolution of chalcopyrite in this work. Similar conclusions were obtained in in the case of bioleaching by *L. ferriphilum*, as shown in Fig. 6(b).
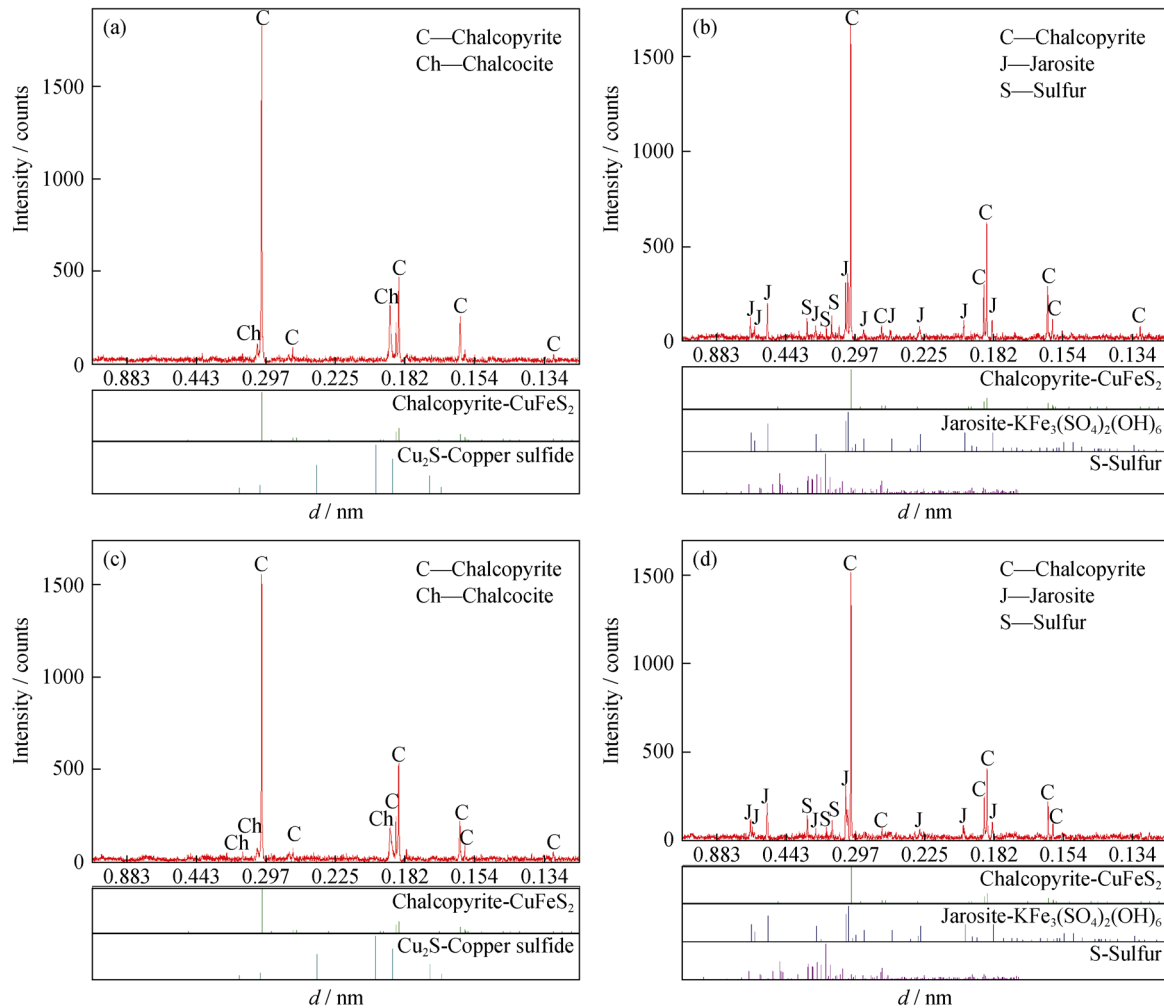
Fig. 5. Mineralogical compositions of a mixture leached for different times in the presence of *A. caldus* and *L. ferriphilum*: (a) 5 d (*A. caldus*); (b) 20 d (*A. caldus*); (c) 5 d (*L. ferriphilum*); (d) 20 d (*L. ferriphilum*).
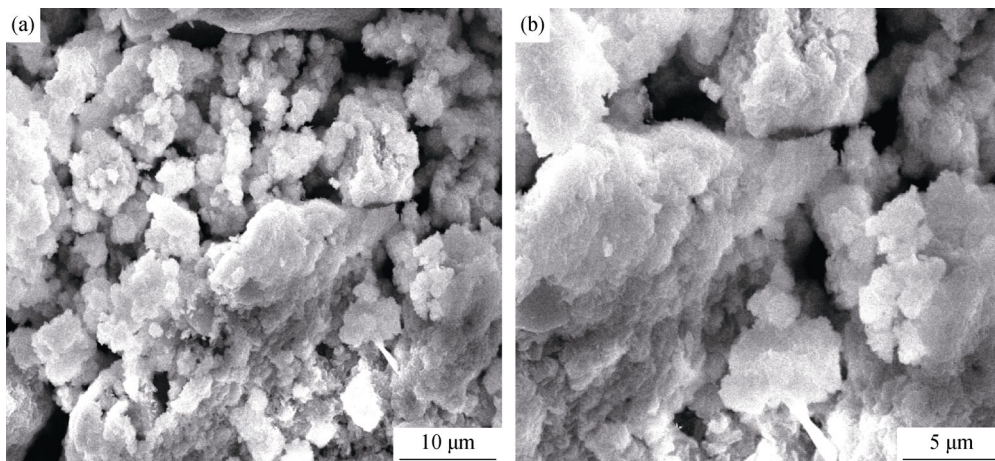

Fig. 6. SEM micrographs of the 1:1 mixture leached for 20 d in the presence of (a) *A. caldus* and (b) *L. ferriphilum.*

3.2. Electrochemical measurements

3.2.1. Electrochemical dissolution process of chalcopyrite and bornite

CV is a widely used electrochemical method for investi-

gating qualitative and semi-quantitative behavior, especially for the analysis of the availabilities of oxidation and reduction reactions. In the positive scan route, scanning started toward the anodic direction, then reversed to the cathodic direction, and finally switched toward the anodic direction

again. In the negative scan route, scanning started toward the cathodic direction, then switched toward the anodic direction, and finally reversed to the cathodic direction. Fig. 7(a) shows that the current density of peak a1 was significantly higher in the negative scan route than in the positive scan route, indicating that the dissolution of chalcopyrite can be accelerated

by the reduction of chalcopyrite. However, the reduction of bornite did not significantly affect its dissolution (Fig. 7(b)).

To characterize the potential range where the oxidation and reduction reactions of chalcopyrite occurred, potentiostatic oxidation and reduction experiments were performed; the results are shown in Fig. 8. The relationship between the
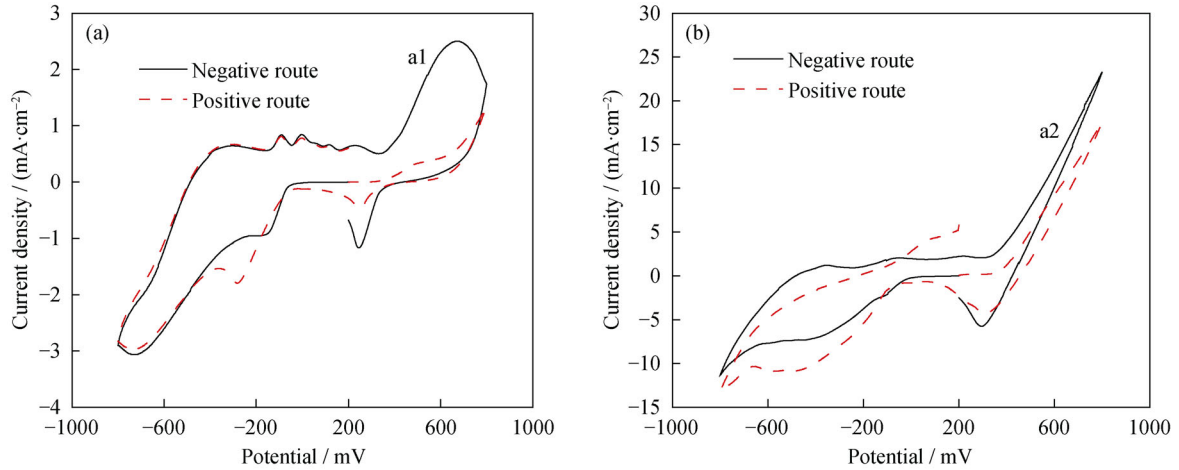

Fig. 7. Cyclic voltammograms of (a) chalcopyrite and (b) bornite electrodes in different scan routes.
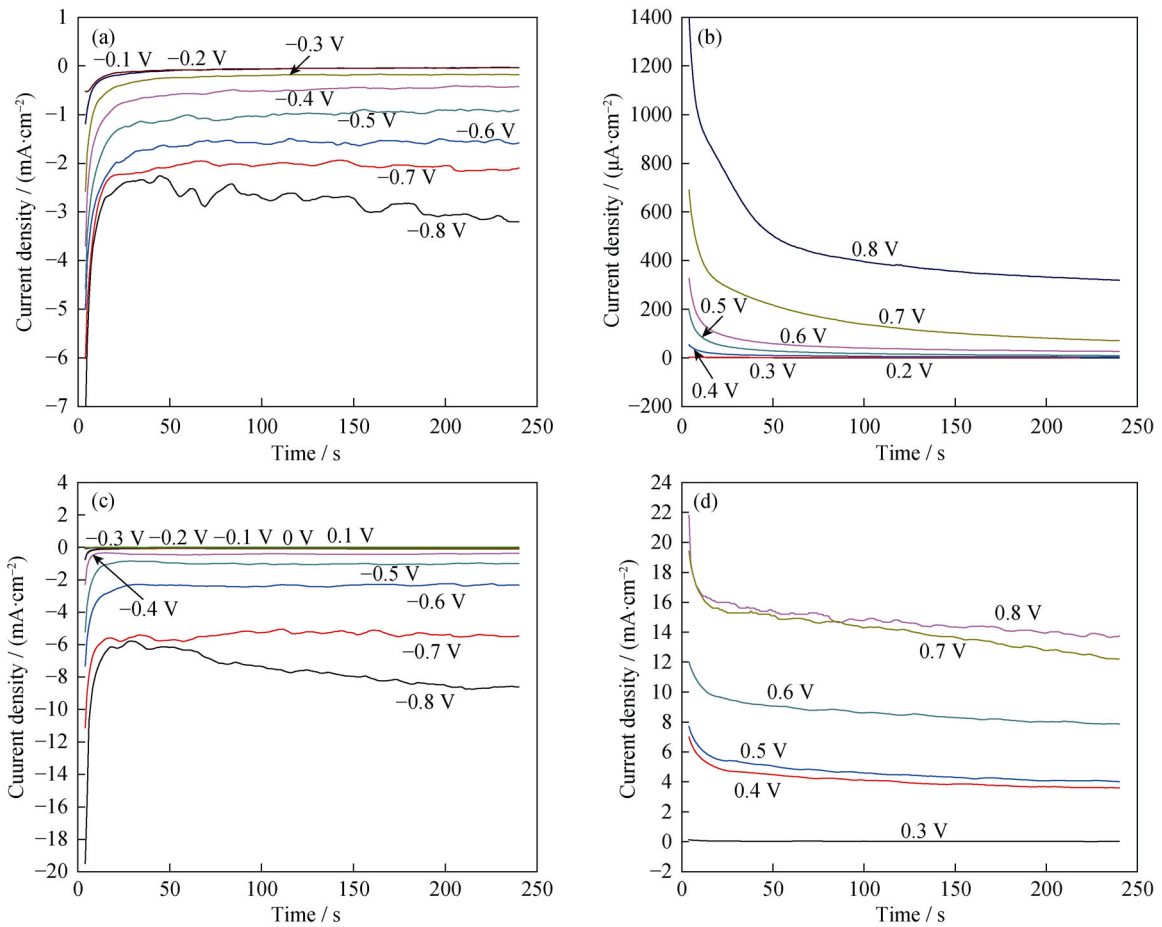

Fig. 8. Current–time curves of chalcopyrite and bornite electrodes at different applied potentials in sterile bacteria culture medium: (a) reduction region of chalcopyrite; (b) oxidation region of chalcopyrite; (c) reduction region of bornite; (d) oxidation region of bornite.
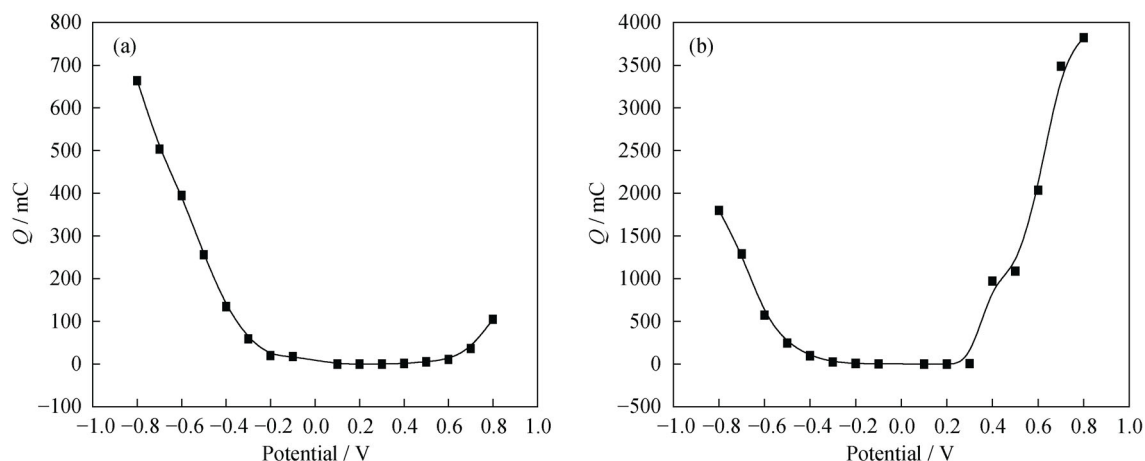
Fig. 9. Relationship between the total charges (evaluated from the current–time curves) and applied potential (*Q* is total charge): (a) chalcopyrite; (b) bornite.

total charge (evaluated from the current–time curves of the chalcopyrite electrode) and the applied potential is shown in Fig. 9, which indicates that chalcopyrite was more prone to reduction than bornite and that bornite was much more easily oxidized than reduced.

3.1.2. Electrochemical interactions between chalcopyrite and bornite

To investigate the electrochemical interactions between chalcopyrite and bornite, we constructed a working electrode as shown in Fig. 10. Two different electrodes were placed together in the new working electrode, and just one side of the electrode (chalcopyrite or bornite electrode) was exposed to the electrolyte. Therefore, one side of chalcopyrite electrode was exposed to the electrolyte when investigating the effects of the bornite electrode on the electrochemical behaviors of the chalcopyrite electrode, and vice versa.

Initially, the potential in the CV tests was scanned from −0.8 V to 0.8 V and then back to −0.8 V. Fig. 11(a) presents the results of CV tests when chalcopyrite electrode was facing with the reference electrode. The two obtained curves were similar, indicating that the presence of bornite did not change the oxidation or reduction process of chalcopyrite. Peak a1 of chalcopyrite was mainly considered as the reduction of chalcopyrite to secondary sulfide species of chalcocite (Cu_2S), as shown in Eq. (2) [27–28]. The peak potential of peak a2 significantly shifted toward the positive direction compared to that of peak a1. Therefore, the presence of bornite did not change the oxidation or reduction reactions of chalcopyrite, but accelerated the reduction of chalcopyrite to secondary sulfide species of chalcocite (Cu_2S). Fig. 11(b) shows the results of CV tests when the bornite electrode was facing the reference electrode. No obvious differences were observed between the two curves, indicat-

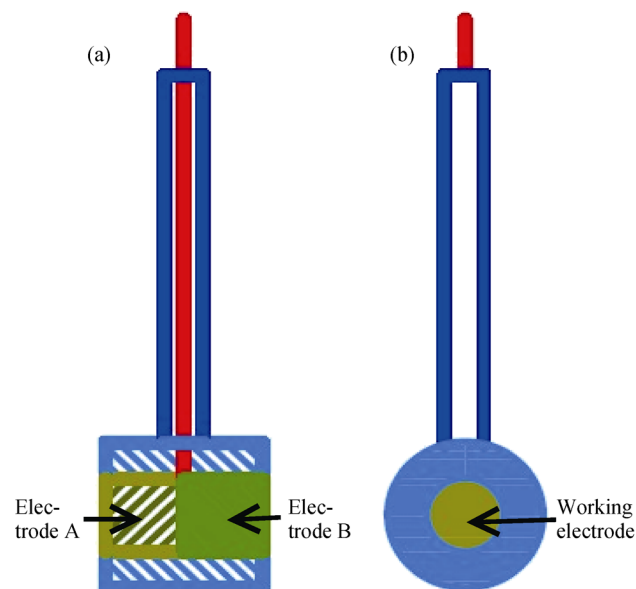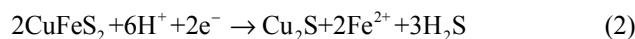ing that the presence of chalcopyrite did not change the oxidation or reduction process of bornite.

Fig. 10. Structure of the working electrode: (a) profile plane; (b) frontal plane.

$$2CuFeS_2 + 6H^+ + 2e^- \rightarrow Cu_2S + 2Fe^{2+} + 3H_2S \qquad (2)$$

Tafel tests can be used to analyze the corrosion kinetics of materials, and the relationship between polarization potential and current density can be described by the Tafel equation. Anodic polarization is described as Eq. (3), and cathode polarization is described as Eq. (4) [29]

$$\eta_a = \psi - \psi_\omega = -\frac{2.3RT}{\beta nF} \lg I_0 + \frac{2.3RT}{\beta nF} \lg I_a \qquad (3)$$

$$\eta_c = \psi_\omega - \psi = -\frac{2.3RT}{\alpha nF} \lg I_0 + \frac{2.3RT}{\alpha nF} \lg I_C \qquad (4)$$

When $|I| \geq I_0$,

$$\eta_a = -\frac{2.3RT}{\beta nF}\lg I_0 + \frac{2.3RT}{\beta nF}\lg I \tag{5}$$

$$I_0 = nFKC_0\left(\frac{C_0}{C_R}\right)^{-a} = nFKC_0^{1-a}C_R^a \tag{6}$$

where η is the polarization overpotential, I_0 is the exchange current density, α and β are the electronic transmission coefficients, K is the electronic reaction rate constant, n is the electron transfer number, C_0 is the concentration of the oxidation product, C_R is the concentration of the reduction product, R is the gas constant, T is the absolute temperature, I_a is the anodic current density, I is the anodic current density in the presence of reductant or oxidant, and F is the Faraday constant.

The value of corrosion potential (E_{corr}) is a parameter that reflects the corrosion resistance abilities of materials; a lower corrosion potential indicates that materials are more easily corroded or oxidized. Fig. 11(c) shows the Tafel polarization curves of the chalcopyrite and bornite electrodes. The corrosion potential of chalcopyrite was higher than that of bornite, indicating that a galvanic cell consisting of chalcopyrite and bornite can form when they coexist. Fig. 11(d) shows the galvanic current density between chalcopyrite and bornite. In the galvanic current tests, a three-electrode system consisting of a chalcopyrite electrode, a reference electrode, and a grounded bornite electrode was used. A current density of approximately 0.6 μA/cm² existed between the cathodic part of chalcopyrite and the anodic part of bornite. The galvanic effect can accelerate the oxidation of the anodic part of bornite and the reduction of the cathodic part of chalcopyrite. Therefore, the galvanic effect is also a potential cause of the synergistic bioleaching of chalcopyrite and bornite, especially during the initial stage of bioleaching.
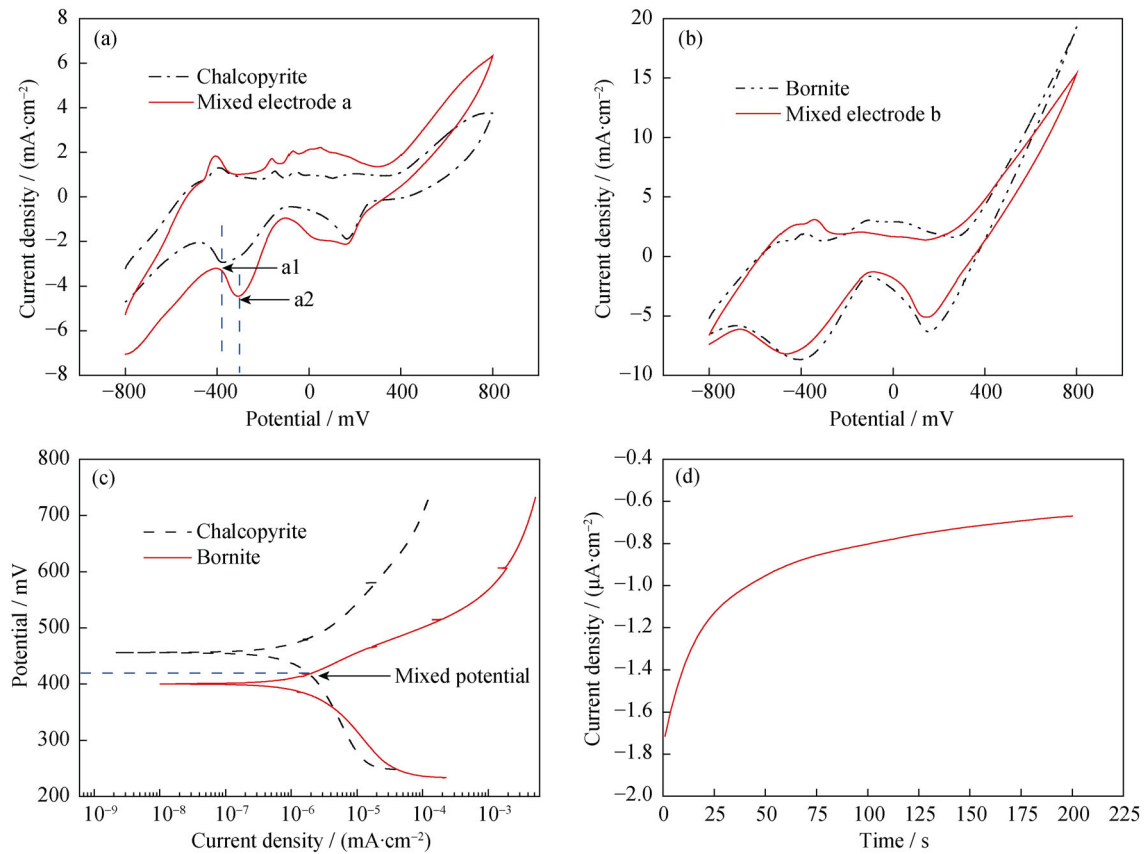

Fig. 11.   Electrochemical behaviors of chalcopyrite and bornite in bacteria culture medium: (a) cyclic voltammograms of chalcopyrite and the mixed electrode; (b) cyclic voltammograms of bornite and the mixed electrode; (c) Tafel curves of chalcopyrite and bornite; (d) galvanic current density.

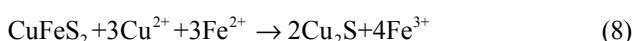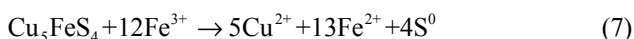### 3.3. Interactions between chalcopyrite and bornite

During the initial stage of bioleaching, bornite dissolved preferentially because of its relatively low corrosion potential. The galvanic current between chalcopyrite and bornite can accelerate the dissolution of bornite, thereby making chalcopyrite more prone to be reduced to the secondary copper sulfide of chalcocite (Cu$_2$S), which dissolves much

786

Int. J. Miner. Metall. Mater., Vol. 22, No. 8, Aug. 2015

easier than chalcopyrite.

The preferential dissolution of bornite can provide a large amount of cupric ions and ferrous ions (Eq. (7)) [30], thus promoting the reduction of chalcopyrite to the secondary copper sulfide of chalcocite (Cu_2S), which is easily dissolved (Eq. (8)) [20–21].

$$Cu_5FeS_4 + 12Fe^{3+} \rightarrow 5Cu^{2+} + 13Fe^{2+} + 4S^0 \quad (7)$$

$$CuFeS_2 + 3Cu^{2+} + 3Fe^{2+} \rightarrow 2Cu_2S + 4Fe^{3+} \quad (8)$$

The Gibbs free energy (ΔG) of the reaction in Eq. (8) is given by

$$\Delta G = \Delta G^{\ominus} + RT \ln \frac{(a Fe^{3+})^4}{(a Fe^{2+})^3 (a Cu^{2+})^3} = -nEF, \quad (9)$$

where R is the gas constant, T is the absolute temperature, a is ionic activity, F is the Faraday constant, and E is the potential of the reaction.

The standard Gibbs free energy ($\Delta G_i^{\ominus}$) of formation for the involved species is shown in Table 1, and the value of the standard Gibbs free energy ($\Delta G^{\ominus}$) of the reaction in Eq. (8) was calculated to be 35.02 kJ/mol. Per the Nernst equation shown in Eq. (1), the standard potential ($E^{\ominus}$) was calculated to be 681 mV vs. SHE (standard hydrogen electrode) or 482 mV vs. Ag/AgCl. This result implies that the reduction reaction in Eq. (8) occurred when the redox potential was lower than 482 mV vs. Ag/AgCl under the standard conditions.

Table 1. Standard Gibbs free energy of formation for the involved species ($\Delta G_i^{\ominus}$) kJ/mol

Cu^{2+}	Fe^{2+}	Fe^{3+}	$CuFeS_2$	Cu_2S
64.98	−84.94	−10.5	−190.6	−86.73

Additionally, the oxidation of chalcocite (Cu_2S) follows the reaction shown in Eq. (10):

$$2Cu_2S \rightarrow 4Cu^{2+} + 2S^0 + 8e^- \quad (10)$$

Similarly, the standard potential ($E^{\ominus}$) was calculated to be 600 mV vs. SHE or 401 mV vs. Ag/AgCl, indicating that chalcocite (Cu_2S) would be oxidized to cupric ions if the redox potential was greater than 401 mV vs. Ag/AgCl.

Therefore, chalcopyrite can be reduced to chalcocite (Cu_2S) and then dissolved into cupric ions if the redox potential is in the range from 401 to 482 mV vs. Ag/AgCl, which is almost in agreement with the results of bioleaching experiments (390–480 mV).

The redox potential of the leaching solution during bioleaching of mixtures can be controlled through numerous factors, including solution composition, complex chemical reactions, and bacterial activity. Further work investigating the factors governing the redox potential of leaching solutions is currently in progress.

4. Conclusions

A synergistic effect was observed between chalcopyrite and bornite in bioleaching by both *A. caldus* and *L. ferriphilum*.

Bornite dissolved preferentially because of its lower corrosion potential. The galvanic current accelerated the dissolution of bornite and made chalcopyrite prone to be reduced to chalcocite (Cu_2S) during the initial stage of bioleaching. Additionally, the dissolution of bornite controlled the redox potential within the range from 390 to 480 mV, which facilitated the reduction of chalcopyrite to chalcocite (Cu_2S), thus accelerating its dissolution.

Acknowledgements

References

[1] K. Koto and N. Morimoto, Superstructure investigation of bornite, Cu_5FeS_4, by the modified partial Patterson function, *Acta Crystall. Sect. B*, 31(1975), No. 9, p. 2268.

[2] P. Baláž, K. Tkáčová, and E.G. Avvakumov, The effect of mechanical activation on the thermal decomposition of chalcopyrite, *J. Therm. Anal.*, 35(1989), No. 5, p. 1325.

[3] J.E. Dutrizac, The kinetics of dissolution of chalcopyrite in ferric ion media, *Metall. Trans. B*, 9(1978), No. 3, p. 431.

[4] H.R. Watling, The bioleaching of sulphide minerals with emphasis on copper sulphides: a review, *Hydrometallurgy*, 84(2006), No. 1-2, p. 81.

[5] Y. Li, N. Kawashima, J. Li, A. Chandra, and A.R. Gerson, A review of the structure, and fundamental mechanisms and kinetics of the leaching of chalcopyrite, *Adv. Colloid Interface Sci.*, 197-198(2013), p. 1.

[6] G. Gu, K. Hu, X. Zhang, X. Xiong, and H. Yang, The stepwise dissolution of chalcopyrite bioleached by *Leptospirillum ferriphilum*, *Electrochim. Acta*, 103(2013), p. 50.

[7] W. Qin, C. Yang, S. Lai, J. Wang, K. Liu, and B. Zhang, Bioleaching of chalcopyrite by moderately thermophilic microorganisms, *Bioresour. Technol.*, 129(2013), p. 200.

[8] C. L. Liang, J. L. Xia, Y. Yang, Z. Y. Nie, X. J. Zhao, L. Zheng, C. Y. Ma, and Y. D. Zhao, Characterization of the thermo-reduction process of chalcopyrite at 65ºC by cyclic voltammetry and XANES spectroscopy, *Hydrometallurgy*, 107(2011), No. 1-2, p. 13.

[9] D. Majuste, V. Ciminelli, K. Osseo-Asare, M. Dantas, and R. Magalhães-Paniago, Electrochemical dissolution of chalcopyrite: detection of bornite by synchrotron small angle X-ray diffraction and its correlation with the hindered dissolution process, *Hydrometallurgy*, 111-112(2012), p. 114.

[10] R.G. Acres, S.L. Harmer, and D.A. Beattie, Synchrotron XPS studies of solution exposed chalcopyrite, bornite, and heterogeneous chalcopyrite with bornite, *Int. J. Miner. Process.*, 94(2010), No. 1-2, p. 43.

[11] M. Gericke, A. Pinches, and J. Van Rooyen, Bioleaching of a chalcopyrite concentrate using an extremely thermophilic culture, *Int. J. Miner. Process.*, 62(2001), No. 1-4, p. 243.

[12] D.A. Clark and P.R. Norris, Oxidation of mineral sulphides by thermophilic microorganisms, *Miner. Eng.*, 9(1996), No. 11, p. 1119.

[13] G.J. Olson, J.A. Brierley, and C.L. Brierley, Bioleaching review part B: progress in bioleaching: applications of microbial processes by the minerals industries, *Appl. Microbiol. Biotechnol.*, 63(2003), No. 3, p. 249.

[14] N.P. Marhual, N. Pradhan, R.N. Kar, L.B. Sukla, and B.K. Mishra, Differential bioleaching of copper by mesophilic and moderately thermophilic acidophilic consortium enriched from same copper mine water sample, *Bioresour. Technol.*, 99(2008), No. 17, p. 8331.

[15] E.M. Córdoba, J.A. Muñoz, M.L. Blázquez, F. González, and A. Ballester, Leaching of chalcopyrite with ferric ion. Part II: Effect of redox potential, *Hydrometallurgy*, 93(2008), No. 3-4, p. 88.

[16] K.A. Third, R. Cord-Ruwisch, and H.R. Watling, Control of the redox potential by oxygen limitation improves bacterial leaching of chalcopyrite, *Biotechnol. Bioeng.*, 78(2002), No. 4, p. 433.

[17] M. Gericke, Y. Govender, and A. Pinches, Tank bioleaching of low-grade chalcopyrite concentrates using redox control, *Hydrometallurgy*, 104(2010), No. 3-4, p. 414.

[18] J. Petersen and D.G. Dixon, Competitive bioleaching of pyrite and chalcopyrite, *Hydrometallurgy*, 83(2006), No. 1-4, p. 40.

[19] A. Ahmadi, M. Schaffie, Z. Manafi, and M. Ranjbar, Electrochemical bioleaching of high grade chalcopyrite flotation concentrates in a stirred bioreactor, *Hydrometallurgy*, 104(2010), No. 1, p. 99.

[20] N. Hiroyoshi, S. Kuroiwa, H. Miki, M. Tsunekawa, and T. Hirajima, Synergistic effect of cupric and ferrous ions on active-passive behavior in anodic dissolution of chalcopyrite in sulfuric acid solutions, *Hydrometallurgy*, 74(2004), No. 1-2, p. 103.

[21] N. Hiroyoshi, H. Miki, T. Hirajima, and M. Tsunekawa, A model for ferrous-promoted chalcopyrite leaching, *Hydrometallurgy*, 57(2000), No. 1, p. 31.

[22] E.M. Córdoba, J.A. Munoz, M.L. Blázquez, F. González, and A. Ballester, Leaching of chalcopyrite with ferric ion. Part IV: The role of redox potential in the presence of mesophilic and thermophilic bacteria, *Hydrometallurgy*, 93(2008), No. 3-4, p. 106.

[23] N. Hiroyoshi, H. Kitagawa, and M. Tsunekawa, Effect of solution composition on the optimum redox potential for chalcopyrite leaching in sulfuric acid solutions, *Hydrometallurgy*, 91(2008), No. 1-4, p. 144.

[24] J. Vilcáez, K. Suto, and C. Inoue, Bioleaching of chalcopyrite with thermophiles: temperature–pH–ORP dependence, *Int. J. Miner. Process.*, 88(2008), No. 1-2, p. 37.

[25] L. Cancho, M. Blázquez, A. Ballester, F. González, and J. Muñoz, Bioleaching of a chalcopyrite concentrate with moderate thermophilic microorganisms in a continuous reactor system, *Hydrometallurgy*, 87(2007), No. 3-4, p. 100.

[26] A. Ahmadi, M. Schaffie, J. Petersen, A. Schippers, and M. Ranjbar, Conventional and electrochemical bioleaching of chalcopyrite concentrates by moderately thermophilic bacteria at high pulp density, *Hydrometallurgy*, 106(2011), No. 1-2, p. 84.

[27] E.M. Arce and I. González, A comparative study of electrochemical behavior of chalcopyrite, chalcocite and bornite in sulfuric acid solution, *Int. J. Miner. Process.*, 67(2002), No. 1-4, p. 17.

[28] A. López-Juárez, N. Gutiérrez-Arenas, and R.E. Rivera-Santillán, Electrochemical behavior of massive chalcopyrite bioleached electrodes in presence of silver at 35°C, *Hydrometallurgy*, 83(2006), No. 1-4, p. 63.

[29] W.Q. Qin, F. Jiao, W. Sun, M.F. He, and H.J. Huang, Selective flotation of chalcopyrite and marmatite by MBT and electrochemical analysis, *Ind. Eng. Chem. Res.*, 51(2012), No. 35, p. 11538.

[30] D. Bevilaqua, O. Garcia Jr., and O. Tuovinen, Oxidative dissolution of bornite by *Acidithiobacillus ferrooxidans*, *Process Biochem.*, 45(2010), No. 1, p. 101.